Catalytic transformations of citral in a continuous flow over bifunctional Ru-MCM-41 extrudates

Vajglová, Zuzana; Mäki-Arvela, Päivi; Eränen, Kari; Kumar, Narendra; Peurla, Markus; Murzin, Dmitry Yu

Published in:
Catalysis Science and Technology

DOI:
10.1039/d1cy00066g

Published: 21/04/2021

Document Version
Accepted author manuscript

Document License
Publisher rights policy

Link to publication

Please cite the original version:
Vajglová, Z., Mäki-Arvela, P., Eränen, K., Kumar, N., Peurla, M., & Murzin, D. Y. (2021). Catalytic transformations of citral in a continuous flow over bifunctional Ru-MCM-41 extrudates. *Catalysis Science and Technology*, *11*(8), 2873-2884. https://doi.org/10.1039/d1cy00066g

Catalytic transformations of citral in a continuous flow over bifunctional Ru-MCM-41 extrudates

Zuzana Vajglová[1], Päivi Mäki-Arvela[1], Kari Eränen[1], Narendra Kumar[1], Markus Peurla[2], Dmitry Yu. Murzin[1*]

[1] *Åbo Akademi University, Johan Gadolin Process Chemistry Centre, Biskopsgatan 8, Turku/Åbo, Finland, 20500*
[2] *University of Turku, Turku, Finland, 20500*
[*] *dmurzin@abo.fi, corresponding author*

Abstract

The three steps reaction of citral to menthol was investigated in an autoclave and a trickle-bed reactor over Ru-MCM-41 catalyst in a powder and shaped forms, respectively, with the same composition, and controlled metal location. All catalysts were characterized in detail and the results were correlated with catalytic tests.

Activity and selectivity were strongly affected by controlling location of Ru in the powder catalyst applied in the batch experiments. The catalyst with the largest distance between the metal and acid sites, and at the same time with the highest total acidity, i.e. with Ru deposited exclusively on a binder Bindzil, displayed the highest yield of menthols. On contrary, in the trickle-bed reactor with extrudates Ru location was of almost no importance which is related to mass transfer. Comparison between batch and continuous experiments also revealed significant differences in the product distribution.

The highest yield of the desired menthol of 6% with stereoselectivity of 66% was obtained at 12.5 min of residence time after 3 h of time-on-stream over egg-shell extrudates with Ru distribution at the outermost layer, deposition of Ru on both H-MCM-41 and the binder Bindzil, and the smallest Ru particle size.

Keywords: citral, menthol, shaped catalyst, metal location, binder, trickle-bed reactor

1 Introduction

Menthol is a fine chemical having the largest global demand among the mint products. It is widely used as a fragrance or flavouring agent in the production of pharmaceuticals, cosmetics, and food products.[1-11] From four diastereoisomeric pairs: (±)-menthol, (±)-neomenthol, (±)-isomenthol, and (±)-neoisomenthol, only (−)-menthol has the physiological cooling effect and the characteristic peppermint odor.[1,3,4,6]

Menthol is produced from natural sources (80%) and by synthetic routes (20%).[2,4,7] New synthetic routes are constantly explored because the current menthol demand cannot be met by menthol production from only natural sources.[7] The selective synthesis of menthol from citral in a one-step process may be a tempting option. Citral is an attractive renewable raw material that can be obtained mainly by distillation of essential oils (lemongrass oil contains ca. 70-80% citral).[3,4,6,8] Another advantage of this process is easy separation and reuse of the heterogeneous catalyst in one step.[12] On the other hand, the direct one-pot synthesis of menthol from citral is also a challenging task requiring bifunctional metal/acid catalysts with the ability to selectively promote several consecutive reaction steps (Figure 1): citral hydrogenation to citronellal, citronellal cyclization to isopulegol, and finally isopulegol hydrogenation to menthol. Additionally there are four different isopulegol and menthol diastereoisomeric pairs, which can be formed in the reaction. These reaction routes are very complex (Figure 1) and it is difficult to control side reactions such as defunctionalization, dehydration and hydrogenolysis, which might be the reason for the lower yields of the desired menthol production.[2,4,7]

Various heterogeneous powder catalysts, such as Pd, Pt, Ir, Os, Ru, Rh, Ni, Co, Cu, Fe on SiO_2,[3,4,13,14] Pd, Ni, Ru, Ir, Pt, Rh, Co on C, Al_2O_3, SiO_2-Al_2O_3, Al-MCM-41, H-MCM-41 or zeolite H-Beta, Zr-Beta, H-Y,[2-4,6,8,15-18] Pd, Ni on hetero-poly acid supported montmorillonite

(HPA-MM),[7] Ir, Pd, Pt on AlF_3,[8] $Ru(bpy)_3$ on saponite materials,[19] bimetallic Pt-Co/C catalyst[15] and supported ionic liquid catalysts[20] have been tested for one-pot synthesis in batch reactor.

These studies revealed that the one-pot transformations of citral to menthol is strongly dependent on the selection of the metal and support pair, and the solvent nature. It was shown that the narrowed *d*-band width of Ru, Ni and Pd compared with other metals decreases the electrostatic repulsion between the metal surface and the conjugated C=C bond of citral, thereby favoring citral adsorption via its C=C bond and subsequently citronellal formation.[4,8] On the contrary, in [3,8,13] was stated that Co, Pt, Os, Ru, and Ir were more selective for C=O hydrogenation. The hydrogenolysis was very prominent on Ir, whereas Pd, Ni, Ru exhibited very low initial hydrogenolysis activity [2]. The highest selectivity to menthol was obtained in the presence of Ni catalyst (65%),[3,4] Pd (51%),[8] Ir (44%)[8] or Ru-based catalysts (9.6%).[8] Strong acidity of the support (ca. > 400 μmol/g) promoted the undesirable side reactions.[2,4,6,21]

Nevertheless, according to our knowledge, there is no study focusing on the one-pot menthol synthesis from citral over shaped catalysts in a continuous mode reported yet in the open literature, despite its industrial attractiveness. It is difficult to avoid mass transfer limitation in continuous mode in industrial condition which leads to significant changes in activity, selectivity, and stability compared to batch operations over powder catalysts.[1,22-25] Moreover the catalyst scale-up process, typically involving a binder synthesis and shaping into the catalyst body, also often leads to different results compared to a pure powder catalyst.[22-34]

The current work builds on our recent study of the one-pot menthol synthesis from (±)-citronellal over Ru-MCM-41 extrudates in a continuous reactor.[1] The main aim is to demonstrate, if Ru-shaped catalyst is a feasible catalyst for producing menthols from combined three steps transformations directly from citral in a trickle-bed reactor. In addition, the work is

focused on the comparison between batch and continuous processes and the influence of the controlled metal location on the mechanism, the product distribution, and catalyst deactivation.

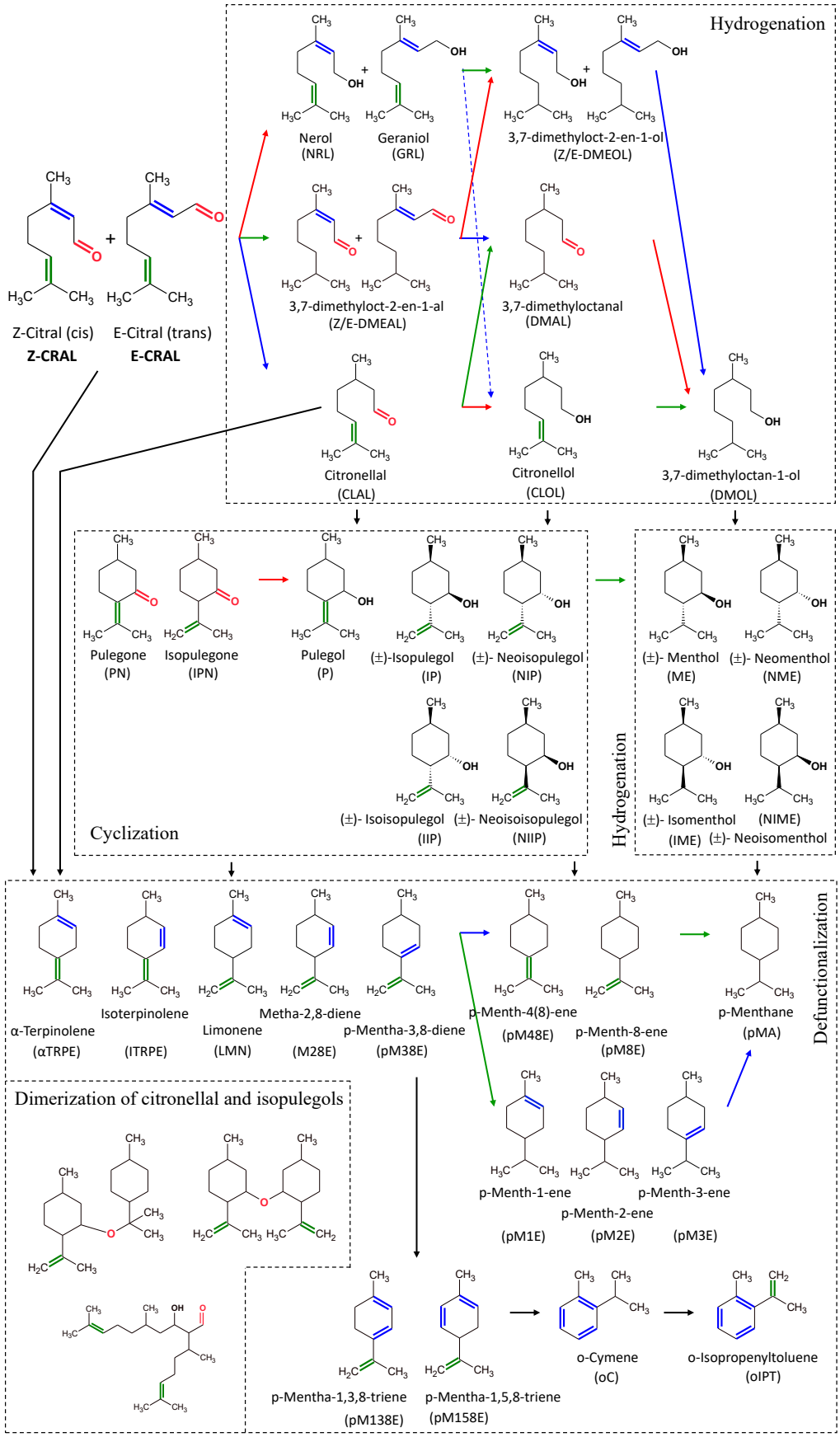

Figure 1. Scheme of menthol synthesis from citral with potential side reactions.

2 Experimental

2.1 Preparation of the shaped Ru-catalysts

The Ru-H-MCM-41-Bindzil catalysts with the same composition but different Ru location were prepared in both powder and extrudates form. For all catalysts, a nominal loading of Ru was 2 wt.% and the weight ratio of H-MCM-41 as a mesoporous catalytic material to Bindzil-50/80 (50% colloidal silica in water from Akzo Nobel) as a binder was 70/30. MCM-41 was prepared at 100 °C for 72 h from a gel solution (fumed silica, scintran, BDH Laboratory; sodium silicate solution, water glass, Merck; cetyltrimethylammonium bromide, 95%, Aldrich; aluminium isopropoxide, 98+%, Aldrich; tetramethylammonium silicate, 15-20% solution in water, Aldrich). Subsequently, the sodium form of the catalyst was transformed into H-MCM-41 by ion exchange with 0.5 M ammonium chloride solution, dried and calcined in a step calcination procedure: 25 °C – 3 °C/min – 250 °C (held for 1 h) and 250 °C – 6.6 °C/min – 550 °C (held for 6 h). Ru was introduced on the catalyst from an aqueous solution of $RuCl_3$ hydrate by the incipient wetness impregnation method. Ru-catalysts were reduced under hydrogen flow at 350 °C for 3 h. Reduction temperature was selected on the basis of the TPR experiments with unsupported ruthenium (oxide) from $RuCl_3$ hydrate,[35] which revealed complete reduction at 267 °C (with a maximum rate of reduction at 202 °C).

Three powder samples were denoted as Ru/(H-MCM-41+Bindzil) (**P-B**), (Ru/Bindzil)+H-MCM-41 (**P-C**), (Ru/H-MCM-41)+Bindzil (**P-D**); where **P** stands for the powder catalyst, **B** for Ru deposition on both H-MCM-41 and Bindzil binder, **C** for Ru deposition exclusively on Bindzil binder, **D** for Ru deposition exclusively on H-MCM-41 mesoporous catalytic material.

The cylindrical-shaped bodies with a diameter of 1.4 mm and length of ca. 10 mm were prepared by extrusion in the one-screw extrusion device (TBL-2, Tianjin Tianda Beiyang Chemical Co. Ltd., China). The catalytic slurry for extrusion contained 33 wt.% of the powder

catalyst, 65 wt.% of distilled water and 2 wt.% of methylcellulose as an organic binder. Selection of the omposition for extrusion was discussed previously.[1] Methylcellulose was burned out from the final extrudates during calcination at 400 °C for 3 h.[1,23,25]

Four extrudates were denoted as Ru/(H-MCM-41+Bindzil) *post* synthesis (**E-A**), Ru/(H-MCM-41+Bindzil) *in-situ* synthesis (**E-B**), (Ru/Bindzil)+H-MCM-41 (**E-C**), (Ru/H-MCM-41)+Bindzil (**E-D**); where **E** stands for extrudates, **A** for Ru distribution at the outermost layer of extrudates (i.e. egg-shell) with Ru deposition on both H-MCM-41 and Bindzil binder, **B** for the uniformly distributed Ru in the entire shaped body with Ru deposition on both H-MCM-41 and Bindzil binder, **C** for the uniformly distributed Ru in the entire shaped body with Ru deposition exclusively on Bindzil binder, **D** for the uniformly distributed Ru in the entire shaped body with Ru deposition exclusively on H-MCM-41 mesoporous catalytic material.

In the current work, the same batch of Ru-catalysts was used as in our previous work focused on citronellal to menthol transformations,[1] where, all details regarding the preparation and characterization of catalysts are described.

2.2 Characterization of Ru-catalysts

Complete characterization of Ru-extrudates was already reported in the previous study.[1] Exactly the same batch of the shaped catalysts, as applied in the current work, therefore, only data for the powder catalysts are presented here. Characterization was performed using the same physico-chemical methods as for extrudates.[1] Textural properties were measured by nitrogen physisorption (Micrometrics 3Flex-3500) using the Dubinin-Radushkevich and density functional theory (DFT) methods for calculations of the specific surface area and pore size distribution, respectively. Morphology of the surface, the particle size and shape of Ru were analysed by transmission and scanning electron microscopy (TEM, JEOL JEM-1400Plus; SEM-EDX, Zeiss Leo Gemini 1530). The metal concentration in the entire volume of the

catalyst was determined by inductively couple plasma – optical emission spectrometry (ICP-OES, PerkinElmer Optima 5300 DV instrument). Details of the physico-chemical characterization methods and equipment are presented in our previous publications.[1,22-26]

2.3 Catalytic tests

All Ru-catalysts were tested in the one-pot cascade transformations of citral to menthol, using powder catalysts or extrudates with 0.086 M of the initial citral (*cis*-/*trans*-isomer ~ 1/1, ≥ 95.0%, Sigma-Aldrich) concentration in cyclohexane (≥ 99.9%, Alfa Aesar) under 70 °C, 10 bar in an autoclave and a trickle-bed reactor, respectively.

The cascade transformations of citral to menthol over powder catalysts was performed in a batch reactor (300 mL) using 0.2 g of the pre-reduced catalyst. Reduction was done *ex-situ* in a glass tube under hydrogen flow of 40 mL/min at 350 °C for 3 h with the heating ramp 2 °C/min. Before a reaction, the reduced catalyst was kept under 10 mL of cyclohexane to avoid oxidation. The total reaction volume was 90.2 mL, whereas 50.2 mL of the solvent with the catalyst was added into the autoclave directly, with the rest of the solvent with the reactant injected into the reactor from the pre-heated vessel after when the reaction conditions in the reactor were achieved. A stirring rate of 1000 rpm was selected to avoid external mass transfer limitations, while the size of catalyst particle below 63 μm was needed to eliminate internal mass transfer resistance.

Influence of the mass transfer limitations, which are an integral part of almost any industrial process, was investigated with Ru-shaped catalysts (10 × 1.4 mm). The experiments were carried out in a trickle-bed reactor (internal diameter and length of the diluted catalyst bed were 12.5 mm and 102 mm, respectively) in a continuous mode.[1,22,23,25] For a better flow distribution throughout the reactor, the catalyst bed contained 1 g of extrudates and 15 g of inert quartz of the size 0.2-0.8 mm. The liquid residence time was 12.5 min at 0.4 mL/min of the feed and 50

mL/min of hydrogen. Ru-shaped catalysts were reduced *in-situ* under the same reduction procedure as described above.

Analysis of the reaction products was carried out using an Agilent GC 6890 N equipped with and FID and DB-1 column (30 m × 250 μm × 0.5 μm). The temperature program consisted of two steps: 110 °C – 0.4 °C/min – 130 °C and 130 °C – 13 °C/min – 200 °C. The temperature of the FID was 340 °C. The products were confirmed with Agilent GC/MS 6890 N/5973 using the same temperature program and the column. Before analysis, the samples were diluted with cyclohexane (solvent).

Definitions are presented in the Supporting Information (SI).

3 Results and Discussion

3.1 Characterization results of Ru-catalyst

In line with the previous literature,[1,22,24] the success of the controlled deposition of Ru on both H-MCM-41 and the binder Bindzil (**A, B**) or exclusively only on the binder (**C**) or H-MCM-41 (**D**) was confirmed by TEM analysis (Figures S1, S2). At the same time, EDX analysis confirmed that extrudates **E-A** prepared *via* the *post* synthesis are of the egg-shell type.[1] SEM analysis pointed out on chemical interactions between the catalyst support and the binder leading physico-chemical properties (Table 1) different from the anticipated ones based on additive contribution of the components.[1,22-26]

Analysis of the Brønsted and Lewis acidity (Table S1) revealed that already shaping H-MCM-41 with the Bindzil binder led to significant changes in acidity. The theoretical value of the total acidity should be ca. 25% higher than the experimentally measured, moreover both amounts of strong Brønsted and Lewis acid sites decreased to almost zero. This also led to a decrease in the ratio of Brønsted to Lewis acidity to 1.2 compared to the theoretical value of

1.48. After introducing Ru, acidity decreased further depending on the support nature. This is in line with the work of Kubička et al.[36] and observations of the authors for Pt-catalysts.[22,24] The changes in the acid sites (Brønsted and Lewis acid sites, and their ratio) after modification with Ru depend on the structure, SiO_2/Al_2O_3 ratio, hydrophobicity and hydrophilicity of microporous zeolites and the mesoporous material MCM-41. Ru nanoparticles deposited on the H-MCM-41 mesoporous material can substitute the Brønsted acid sites, thereby decreasing acidity.

Different options for controlled deposition of Ru led, besides variations of acidity in the final catalysts (44-69 μmol/g, Table 1), also to different particle sizes of Ru (7-20 nm, Table 1) and slightly different metal concentrations in the entire catalyst volume (0.9-1.4, Table 1). Related to this, the metal-to-acid site ratio (c_{Ru}/c_{AS} = 0.09-0.29, Table 1) was not the same for the catalyst with the same composition (70% of H-MCM-41 and 30% of Bindzil) and the same metal nominal loading (2 wt.% of Ru), which is in line with the literature.[1,22,24] However, it should be noted that acidity of the final extrudates was similar for all types.

Table 1. Characterization results of powder and shaped Ru-catalysts with the controlled metal location. In parenthesis data for the spent catalysts. Legend: TAS – total acid sites; BAS – Brønsted acid sites; LAS – Lewis acid sites; *B/L – ratio of Brønsted and Lewis acid sites; d_{Ru} – Ru particle size; D_{Ru} – metal dispersion (100/d_{Ru}); c_{Ru_E} – Ru concentration on the top of extrudates surface; c_{Ru} – Ru concentration in the entire volume; A – specific surface area; V_p – specific pore volume; $V_{\mu p}$ – micropore volume; c_{AS} – concentration of total acid sites.*

Cat.	c_{Ru}/c_{AS}	TAS	BAS	LAS	B/L	d_{Ru}	D_{Ru}	c_{Ru_E}	c_{Ru}	A	V_p	V_μ
	-	*μmol/g*			-	*nm*	*%*			*m^2/g*	*cm^3/g*	
P-B	0.26	65	21	44	0.5	8	13	-	1.4	440 (329)	0.62 (0.39)	0.12 (0.09)
P-C	0.09	69	37	32	1.1	20	5	-	1.3	496 (400)	0.54 (0.48)	0.13 (0.11)
P-D	0.20	44	28	15	1.9	12	8	-	1.1	528 (458)	0.37 (0.55)	0.14 (0.12)
E-A [1]	0.29	60	37	24	1.5	7	14	8.8	1.2	483 (361)	0.65 (0.74)	0.14 (0.08)
E-B [1]	0.17	51	31	21	1.5	13	8	1.2	1.2	514 (383)	0.72 (0.73)	0.14 (0.09)
E-C [1]	0.14	60	35	25	1.4	11	9	0.3	0.9	502 (365)	0.67 (0.65)	0.14 (0.09)
E-D [1]	0.23	52	29	22	1.3	10	10	1.6	1.2	520 (399)	0.71 (0.72)	0.14 (0.09)

P – powder catalyst; E - extrudates; **P-B** – Ru/(H-MCM-41+Bindzil); **P-C** – (Ru/Bindzil)+H-MCM-41; **P-D** – (Ru/H-MCM-41)+Bindzil; **E-A** – Ru/(H-MCM-41+Bindzil) *post* synthesis; **E-B** – Ru/(H-MCM-41+Bindzil*) in-situ* synthesis; **E-C** – (Ru/Bindzil)+H-MCM-41; **E-D** – (Ru/H-MCM-41)+Bindzil.

The results of textural properties revealed by ca. 18% and 32% lower measured values of the specific surface area and micropore volume, respectively were obtained, compared to the theoretical values for the mechanical mixture (A = 605 m^2/g, V_μ = 0.2 cm^3/g). Similar results were observed in the literature.[1,23-26] After the reaction, the specific surface area and micropore volume decreased again by ca. 23% and 30%, respectively. By comparison of the pore size distribution of the fresh and spent catalysts (Figure 2), it can be concluded that during the reaction the pores of catalyst are blocked. Distribution of the mesopores was shifted from a larger pore size to the smaller ones, which could be related to coke formation.[1,2]

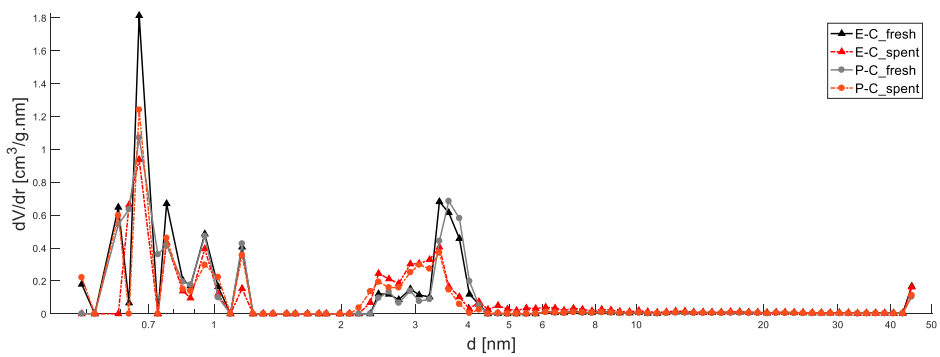

*Figure 2. Pore size distribution of (Ru/Bindzil)+H-MCM-41 catalysts. Legend: fresh powder catalyst (**P-C**_fresh), spent powder catalyst (**P-C**-spent), fresh extrudates (**E-C**_fresh), spent extrudates (**E-C**_spent).*

The colloidal silica (Bindzil-50/80) was used as a non-acidic inorganic binder without impurities in order to avoid any potential interference of the binder with the catalytic reactions influencing the reaction network.[1,22,23] However, in line with the literature,[26,28-31] the characterization results confirmed binder–catalyst interactions exerting the catalytic performance through both physical and chemical reasons. The binder presence can thus lead to a marked influence on activity, selectivity, and stability of a catalyst.

3.2 Activity and selectivity of powder Ru-catalysts in the batch experiments

Figures3-7 display the catalytic results of citral transformations over Ru powder catalysts in the batch reactor. For all powder catalysts with a controlled Ru location, the initial concentration profiles with the normalized time (SI), taking into account the catalyst mass, concentration and the particle size of ruthenium, are almost the same (Figure 3). However, after the first hour, significant deactivation was observed with the catalyst **P-D** with the medium particle size of ruthenium (12 nm, Table 1). In the case of Z-citral isomer, the concentration decreased in the fastest way for the catalyst **P-C** with the largest Ru particle size (20 nm, Table 1). The concentration profile of E-citral isomer was the same for **P-B** and **P-C** catalysts. Overall, it can be concluded that structure sensitivity in citral hydrogenation is independent on the particle size of ruthenium. The primary data of citral concentration profile are reported in the Supporting Information (Figure S3).

Such concentration profiles clearly indicate that rates and thus turn-over-frequency (TOF) depend on the reaction time (Table S2, Figure S3d, Figure 4a). After 3 h, the highest values of instantaneous (TOF_{inst} = 0.07 s^{-1}) and cumulative TOF (TOF_{cum} = 0.25 s^{-1}) were determined for the catalyst **P-C**. Cumulative TOF is calculated as reacted moles per time interval (time t – time zero) divided by moles of exposed measured metal. In the case of instantaneous TOF, the time interval was from time t-1 to time t. Definitions are presented in the Supporting Information.

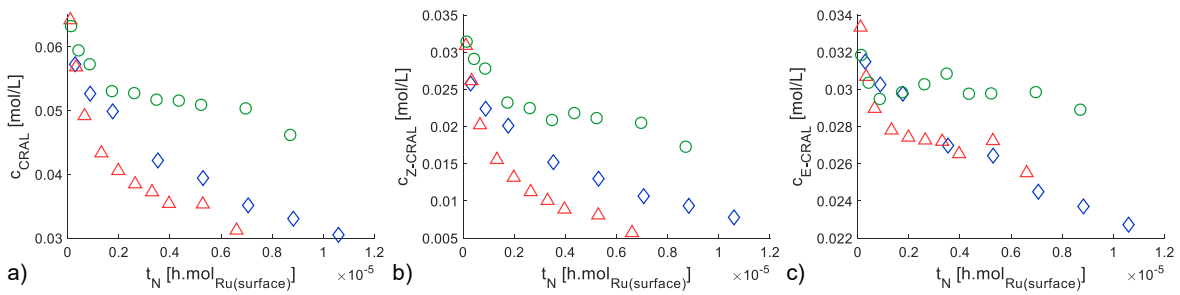

*Figure 3. Concentration profiles as a function of normalized time: a) racemic mixture of citral, b) Z-citral, c) E-citral. Legend: Ru/(H-MCM-41+Bindzil) (**P-B**, dark blue diamond), Ru/(Bindzil)+H-MCM-41 (**P-C**, red triangle),*

*Ru/(H-MCM-41)+Bindzil (**P-D**, green circle). Conditions: 70 °C, 10 bar of H_2, 0.086 M initial concentration of citral in cyclohexane, 0.2 g of catalyst.*

Conversion of citral as a function of normalized time revealed a significant difference between catalysts with a controlled Ru location (Figure 4b). These differences clearly correlate with the total acidity (Figure S4a) and can be also attributed to the proximity between the metal and acid sites (Figure S5). In other words, the highest conversion of citral (58% after 5 h, i.e. $7 \cdot 10^{-6}$ $h \cdot mol_{Ru(surface)}$) was achieved for the catalyst **P-C** with Ru deposited on the binder Bindzil, i.e. with the largest distance between the metal and acid sites, and at the same time with the highest total acidity. The liquid phase mass balance closure (MB, Figure 4c) was similar for all powder catalysts being ca. 80%. The same MB was also observed for citronellal transformations to menthol over Ru-catalysts.[1] The total yield (Figure 4d) was the lowest for the catalyst **P-D** with the highest B/L ratio (Figure S4b), rather large Ru particle size and Ru deposited on H-MCM-41, which may be related to the shortest distance between the metal and acid sites. Observed deactivation of the **P-D** catalyst and a low MB (ca. 75%) could be attributed to the large amount of oligomers because of slow hydrogenation and isomerization in presence of a catalyst with a high B/L ratio.

In comparison with the literature, a similar conversion of citral (55%) was achieved over 0.05 g of 3 wt.% Ru/Beta powder catalyst after a longer reaction time of 24 h at 100 °C and 10 bar of H_2 [8]. Contrary, after a similar time (5.5 h), a significantly higher citral conversion of 95% was observed over 0.3 g 5 wt.% Ru/H-MCM-41 with a higher metal loading and without the presence of a binder Bindzil at the same temperature (70 °C) and pressure (10 bar H_2) compared to the current work [2].

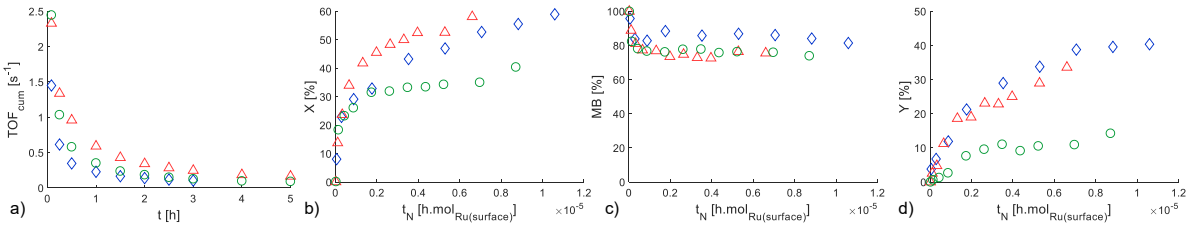

*Figure 4. Citral transformations over Ru powder catalyst in the batch reactor: a) cumulative turn-over-frequency as a function of reaction time; b) conversion of citral, c) liquid phase mass balance (MB) closure, d) total yield as a function of normalized time. Legend: Ru/(H-MCM-41+Bindzil) (**P-B**, dark blue diamond), Ru/(Bindzil)+H-MCM-41 (**P-C**, red triangle), Ru/(H-MCM-41)+Bindzil (**P-D**, green circle). Conditions: 70 °C, 10 bar of H_2, 0.086 M initial concentration of citral in cyclohexane, 0.2 g of catalyst.*

For all powder catalysts, low total yields of acyclic hydrogenation products (0.5% to 4.5%, Figure 5a) including citronellal (CLAL) were observed. For catalysts **P-B** and **P-C**, 3,7-dimethyloctan-1-ol (DMOL), geraniol (GRL) and citronellol (CLOL) were also detected amount the products. The distribution of acyclic products is in line with the literature[3,4,8,14] where it was stated that Ru with the narrowed *d*-band of 4.9 eV favors C=C bond hydrogenation forming citronellal and, subsequent hydrogenation to citronellol or 3,7-dimethyloctan-1-ol. On the contrary, over 0.75% Ru/SiO_2 powder catalyst mainly geraniol+nerol with 56% selectivity along with citronellal (27%) and isopulegol (17%) at citral conversion of 5% after 2.8 h at 27 °C and atmospheric pressure[13] were obtained.

Overall, in the current work, in all cases, the main products of the reaction were defunctionalization products (ca. 8-20% Figure 5b, Figure S6), namely p-mentha-1,3,8-triene (Y_{pM138E}=5-11%) and p-mentha-1,5,8-triene (Y_{pM158E}=1.5-4.5%). A similar result was observed in the literature[2] over 5 wt.% Ni/H-MCM-41 powder catalyst without a binder, where 40% of hydrogenolysis products were formed after 5.5 h with menthatrienes as the main hydrogenolysis products.

The highest yield of isopulegols (13%) was observed for the catalyst **P-B** with random Ru distribution on both H-MCM-41 and the Bindzil binder (Figure 5c). On the other hand, the

highest yield of menthols (2.8%) was detected for the catalyst **P-C** with Ru deposited exclusively on a binder Bindzil with the longest distance between metal and acid sites and with the highest total acidity (Figure 5d). This led to a different ratio of isopulegols to menthols: **P-B** (7.2) > **P-D** (3.9) > **P-C** (1.9). As a comparison with the literature[2], selectivity to isopulegol of 13% and IP/ME ratio of 3.3 were obtained at 50% citral conversion with 5 wt.% Ru/H-MCM-41.

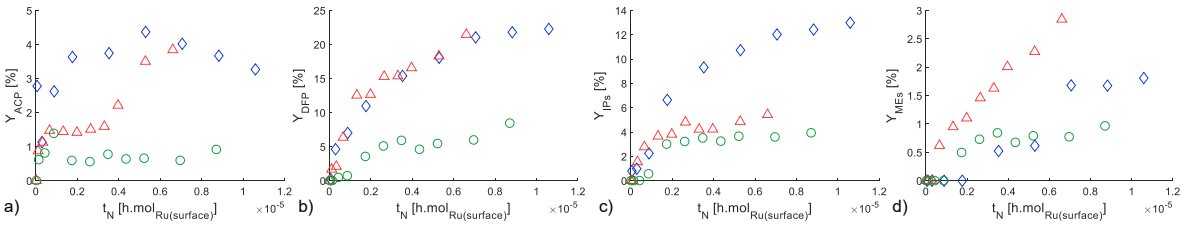

*Figure 5. Product distribution in citral transformations over Ru/(H-MCM-41+Bindzil-50/80) powder catalyst in the batch reactor: a) yield of acyclic hydrogenation products, b) yield of defunctionalization products, c) yield of isopulegols, d) yield of menthols as a function of normalized time. Legend: Ru/(H-MCM-41+Bindzil) (**P-B**, dark blue diamond), Ru/(Bindzil)+H-MCM-41 (**P-C**, red triangle), Ru/(H-MCM-41)+Bindzil (**P-D**, green circle). Conditions: 70 °C, 10 bar of H_2, 0.086 M initial concentration of citral in cyclohexane, 0.2 g of catalyst.*

The detailed analysis of isopulegols (Figure 6, Table S3) revealed significantly differences of isomers distribution as was already shown in citronellal transformations over Ru-catalysts with controlled metal location.[1] In general, in citronellal transformations, significant higher (±)-isopulegol stereoselectivity was achieved with Lewis acids catalysts (ca. 90-94%, $ZnBr_2$ or Zr-Beta) [10,37,38] while stereoselectivity close to the thermodynamic equilibrium (ca. 70-75% for (±)-isopulegol) was observed over an acid solid zeolitic catalyst.[5,10-12,36,38] In the current work, isopulegol (IP) as the major isomer (Y_{IP} = 7%) was observed only over the catalyst **P-B** with the highest amount of Lewis acid sites and a random Ru deposition on both H-MCM-41 and the Bindzil binder (Figure S4c). The isopulegol stereoselectivity split was 54%:33%:14% of isopulegol (IP):neoisopulegol (NIP): isoisopulegol (IIP), while for catalysts with controlled

deposition of Ru (catalysts **P-C** and **P-D**), the major isopulegol isomer was neoisopulegol (Y_{NIP} = 3.6% and 1.8%, respectively). It could be related to a high ratio of Brønsted to Lewis acid sites (B/L >1, Table 1, Figure S4d).

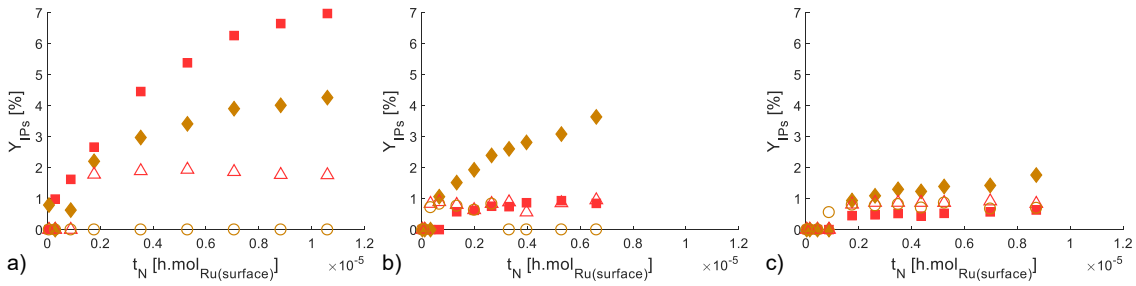

*Figure 6. Isopulegol isomers as a function of normalized time in citral transformations over Ru/(H-MCM-41+Bindzil-50/80) powder catalyst in the batch reactor: a) Ru/(H-MCM-41+Bindzil) (**P-B**), b) Ru/(Bindzil)+H-MCM-41 (**P-C**), c) Ru/(H-MCM-41)+Bindzil (**P-D**). Conditions: 70 °C, 10 bar of H_2, 0.086 M initial concentration of citral in cyclohexane, 0.2 g of catalyst. Legend: isopulegol (red, filled square), neoisopulegol (orange, filled diamond), isoisopulegol (red, empty triangle), neoisoisopulegol (orange, empty circle).*

It is noteworthy that also the distribution of menthol isomers was not the same for all powder catalysts (Figure 7, Table S4). Among the isomers isomenthol was the main one (Y_{IME} /Y_{MEs} = 44-100%). The desired menthol was formed only over **P-B** (Y_{ME} = 0.4%, the highest amount of Lewis acid sites) after 2 h and **P-C** (Y_{ME} = 0.6%) after 5 h. Formation of isomenthol as the main isomer is contrary to the literature[2-4,6] where only menthol was reported as the dominant product. This result could be related to a different distribution of the four isopulegol diastereomers formed in the previous step and different rates of the isopulegol isomers hydrogenation to menthol isomers. The stereoselectivity of menthol:neomenthol:isomenthol:neoisomenthol was (70-72):(20-25):(4-8):(0-4) for Ni on Beta, Al-MCM-41, H-MCM-41, SiO_2-Al_2O_3 catalysts[2-4,6] and 47:16:37 for Pd on Beta catalyst.[3] The difference between the ratio of menthol isomers over Pd- and Ni/Beta catalysts was explained by formation of DMOL on Pd.[3]

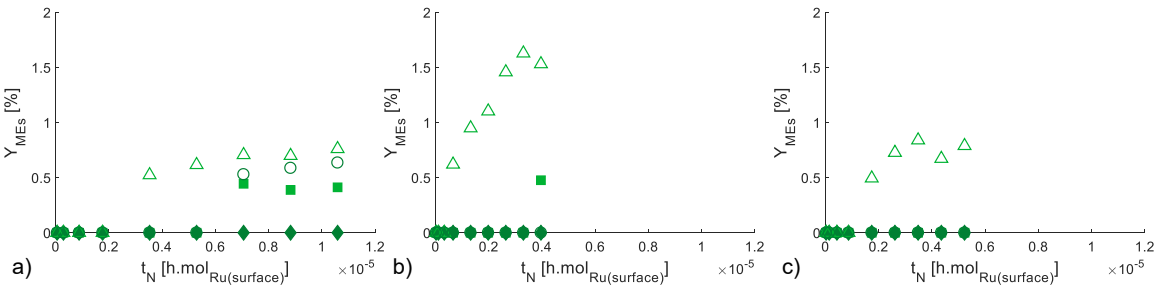

*Figure 7. Menthol isomers as a function of normalized time in citral transformations over Ru/(H-MCM-41+Bindzil-50/80) powder catalyst in the batch reactor: a) Ru/(H-MCM-41+Bindzil) (**P-B**), b) Ru/(Bindzil)+H-MCM-41 (**P-C**), c) Ru/(H-MCM-41)+Bindzil (**P-D**). Conditions: 70 °C, 10 bar of H_2, 0.086 M initial concentration of citral in cyclohexane, 0.2 g of catalyst. Legend: menthol (light green, filled square), neomenthol (dark green, filled diamond), isomenthol (light green, empty triangle), neoisomenthol (dark green, empty circle).*

3.3 Activity and selectivity of shaped Ru-catalysts in the continuous experiments

Experiments with shaped Ru-catalysts in the trickle-bed reactor revealed significantly different behavior in citral transformations to menthol compared to the batch experiment with powder Ru-catalysts. This is attributed to the presence of the diffusion regime confirmed by comparison of cumulative TOF and reaction rates over powder and shaped catalysts (Table S2). The effectiveness factor for extrudates was calculated to be 0.18 – 0.29 (Table S2, $\eta = r_{extrudates}/r_{powder\_catalyst}$).

The highest values of cumulative turn-over-frequency (TOF) were observed for **E-B** and **E-C** catalysts while for the egg-shell extrudates **E-A** the lowest TOF was observed (Table S2, Figure 8). A lower liquid phase mass balance closure (MB, by ca. 17%) and the total yield (by ca. 18%) were observed for extrudates **E-C** compared to other extrudates. The profile of these parameters as a function of the time-on-stream was similar for all extrudates (Figure 8).

The results showed that the catalysts were not stable and continuous deactivation has occurred at about the same rate. A comparable conversion of citral was observed after 3 h of TOS (64 – 70%). A significantly different deactivation pattern was obtained when (±)-citronellal was used as a substrate.[1] In the literature[1] it was observed that the citronellal conversion was after 3 h of TOS ca. 86% and 95% for random (**E-A**, **E-B**) and selective Ru

deposition on extrudates (**E-C**, **E-D**), respectively. Significantly higher deactivation rate in citral hydrogenation could be related to formation of higher amount of terpenic compounds (Figure S7), which can deactivate catalyst in comparison to the citronellal case.

In both cases, the experiments confirmed a complicated reactor dynamics showing stable behaviour of the total yield after ca. 1.5-2 h (Figure 8d).[1]

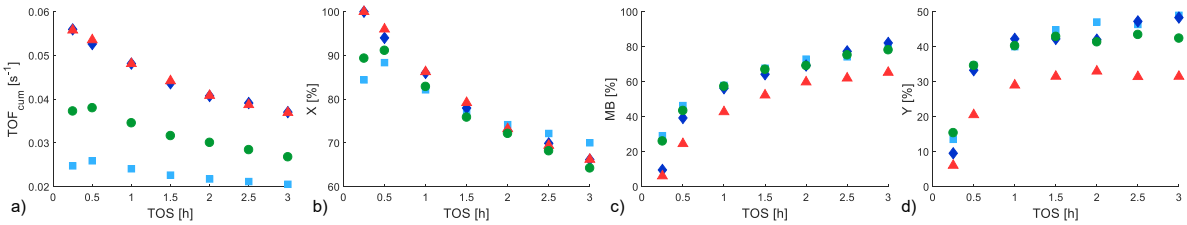

*Figure 8. Citral transformations over Ru/(H-MCM-41+Bindzil-50/80) extrudates in the trickle-bed reactor: a) cumulative turn-over-frequency, b) conversion of citral, c) liquid phase mass balance closure, d) total yield as a function of time-on-stream (TOS). Legend: Ru/(H-MCM-41+Bindzil), post synthesis (**E-A**, light blue square), Ru/(H-MCM-41+Bindzil), in-situ synthesis (**E-B**, dark blue diamond), Ru/(Bindzil)+H-MCM-41 (**E-C**, red triangle), Ru/(H-MCM-41)+Bindzil (**E-D**, green circle). Conditions: 70 °C, 10 bar of H_2, 0.086 M initial concentration of citral in cyclohexane, 1 g of catalyst, 12.5 min of residence time.*

Figure 9 clearly shows that the effect of the controlled Ru location on selectivity in citral transformations to menthol is negligible compared to the effect of internal mass transfer resistance for consecutive reactions. In the case of powder catalysts, the highest yield of menthols was achieved over the catalyst **P-C** with Ru deposited exclusively on the Bindzil binder, i.e. with a longer distance between acid and metal sites (Figure 5). For extrudates with the uniformly distributed Ru in the entire shaped body and controlled Ru deposition (**E-B**, **E-C**, **E-D**), the selectivity was very similar. On the contrary, significant differences in selectivity were observed for the egg-shell type extrudates **E-A** with Ru distribution at the outermost layer of extrudates, random Ru deposition on both H-MCM-41 and Bindzil binder and the smallest Ru particle size (7 nm, Table 1). Over shaped catalyst **E-A**, ca. 4-fold, 20-fold and 1.5-fold times higher yield of menthols, acyclic hydrogenation products and isopulegols, respectively,

(Figure 9), and at the same time, ca. 2.5-fold times lower yield of p-menthatrienes (Figure S7) were obtained compared to other extrudates (Table S5, S6). This catalyst exhibits the highest Ru dispersion (Table 1) among all studied extrudates, while acidity was comparable.

As in the case of the powder catalysts, the defunctionalization products constituted the major part of the reaction mixture (ca. 25-35%). However, the highest initial concentration was detected not for p-mentha-1,3,8-triene and p-mentha-1,5,8-triene, but for p-menthane in a continuous reactor (Figure S7). p-Menthane is formed on a catalyst active in hydrogenation (Figure 1). The concentration of p-menthane decreased with TOS to zero (from ca. Y_{pMA} = 20-25%) while the concentration of p-menthatrienes increased (from Y_{TE} = 0-2% to Y_{TE} = 18-20% in 3 h of TOS) for extrudates with the uniformly distributed Ru in the entire shaped body (**E-B**, **E-C**, **E-D**). Changes in the product composition and selectivity are clearly related to catalyst deactivation and subsequently lower conversion. The results also indicate that mass transfer limitation has a higher effect on the acid-base catalysed reaction than on hydrogenation.

For the egg-shell type extrudates **E-A**, after 3 h of TOS the concentration of p-menthane was still higher than the concentration of p-menthatrienes, which, on the contrary, increased with TOS (Figure S7, Table S6). Worth noting that p-menthane was the main compound amoung the defunctionalization products in (±)-citronellal transformations over Ru containing extrudates.[1] However, the yield of p-menthane was ca. 5-fold lower and the maximum was observed at a longer time (ca. 1 h of TOS) compared to the citral case. Overall, p-menthatrienes were formed more rapidly from citral than from citronellal.[1]

As mentioned above, a significant amount of acyclic hydrogenation products (ACP) were observed only with extrudates **E-A** with the highest dispersion (Figure 9a, Table S5, S6). The major component was 3,7-dimethyloctan-1-ol (Y_{DMOL} = 3.1% at 3 h of TOS) which was the only ACP product obtained over extrudates **E-C** with Ru located exclusively on the Bindzil

binder (Y_{DMOL} < 1.5% with a maximum at 2 h of TOS) indicating efficient hydrogenation activity of Ru on a mildly acid support and with the longest distance between the metal and acid sites (Figure S7). On the contrary, in the case of **E-B** and **E-D** extrudates, only a dehydration product of DMOL, 2,6-dimethyloctane (Y_{DME} < 1.2) with a maximum at 0.3 h of TOS was detected among ACP (Figure S7).

Citronellal (Y_{CLAL} = 0.5 – 3%, Figure S6) obtained with powder catalysts was detected only over extrudates **E-A** after 3 h of TOS with a very low yield (Y_{CLAL} = 0.6 %, Figure S7, Table S6). It should be also pointed out that dimeric ethers and heavy components were observed only over extrudates **E-B** (Y_{DM} = 9.4%) and **E-D** (Y_{DM} = 4.4%) (Table S6). Since Ru distribution, Ru particle size and acidity of the catalysts were comparable with extrudates **E-C**, it can be assumed that the short distance between the metal and acid sites in combination with the diffusion regime had a strong effect on the formation of ethers.

Overall, the largest differences in the product distribution caused by the scale-up of catalysts (1 g of extrudates from a powder catalyst) were observed for citronellal (CLAL) formation occurring in higher concentrations only in the presence of powder catalysts contrary to 3,7-dimethyloctan-1-ol (DMOL) and p-menthane (pMA), which were detected in higher concentrations only over extrudates. Formation of other acyclic hydrogenation and defunctionalization products was only marginally affected by mass transfer (Table S6, Figure S5, S6).

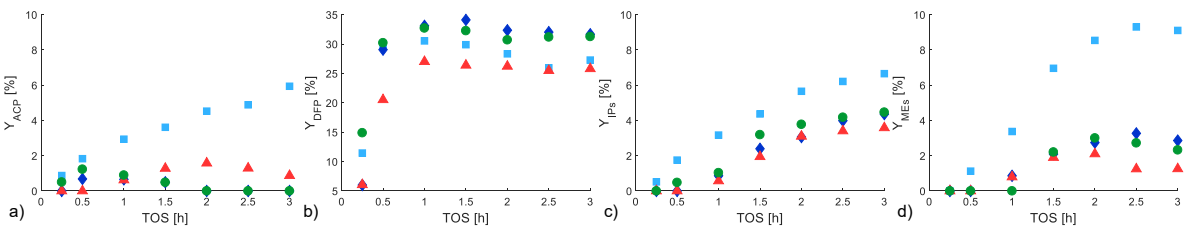

Figure 9. Product distribution in citral transformations over Ru/(H-MCM-41+Bindzil-50/80) extrudates in the trickle-bed reactor: a) yield of acyclic hydrogenation products, b) yield of defunctionalization products, c) yield of isopulegols, d) yield of menthols as a function of time-on-stream. Legend: Ru/(H-MCM-41+Bindzil), post

*synthesis (**E-A**, light blue square), Ru/(H-MCM-41+Bindzil), in-situ synthesis (**E-B**, dark blue diamond), Ru/(Bindzil)+H-MCM-41 (**E-C**, red triangle), Ru/(H-MCM-41)+Bindzil (**E-D**, green circle). Conditions: 70 °C, 10 bar of H_2, 0.086 M initial concentration of citral in cyclohexane, 1 g of catalyst, 12.5 min of residence time.*

As already mentioned above for the powder catalyst and in the literature[1] for extrudates with controlled Ru location significantly different isopulegol stereoselectivity was observed in citronellal transformations. The same was noticed for citral transformations over extrudates even though acidity of the extrudates was quite similar to each other (Table 1, Figure 10, Table S3). Similar stereoselectivity (ca. 55%:35%:10% of IP:NIP:IIP) was observed only for **P-B**, **E-A** and **E-B** catalysts with random Ru deposition on both H-MCM-41 and Bindzil in ciral transformations. The highest yield of isopulegol (Y_{IP} = 3.7%) as the major isopulegol isomer was achived over extrudates **E-A** with the highest dispersion. In the case of extrudates **E-C** with Ru deposited exclusively on the Bindzil binder, neoisopulegol (Y_{NIP} = 1.9%) was detected as the major isopulegol isomer with low interactions between Ru-acid sites. In the case of **E-D** extrudates with Ru deposited exclusively on H-MCM-41 and the shortest distance between metal to acid sites, the stereoselectivity of isopulegol and neoisopulegol was the same (42%).

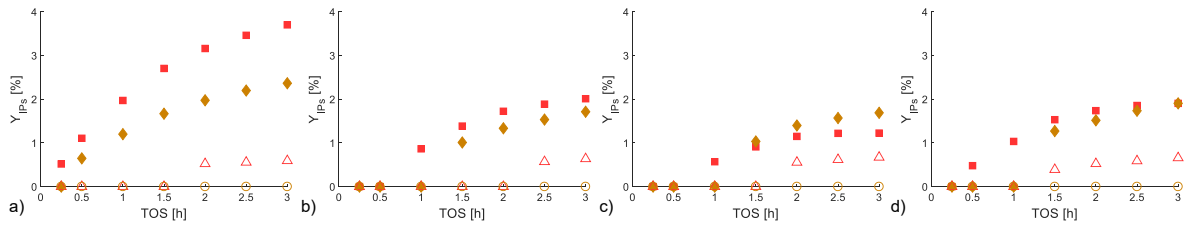

*Figure 10. Isopulegol isomers as a function of time-on-stream in citral transformations over Ru/(H-MCM-41+Bindzil-50/80) extrudates in the trickle-bed reactor: a) Ru/(H-MCM-41+Bindzil), post synthesis (**E-A**), b) Ru/(H-MCM-41+Bindzil), in-situ synthesis (**E-B**), c) Ru/(Bindzil)+H-MCM-41 (**E-C**), d) Ru/(H-MCM-41)+Bindzil (**E-D**). Conditions: 70 °C, 10 bar of H_2, 0.086 M initial concentration of citral in cyclohexane, 1 g of catalyst, 12.5 min of residence time. Legend: isopulegol (red, filled square), neoisopulegol (orange, filled diamond), isoisopulegol (red, empty triangle), neoisoisopulegol (orange, empty circle).*

The absolutely highest yield of the desired menthol of 6% with stereoselectivity of 66% was obtained in the current work over the egg-shell extrudates **E-A** with the highest dispersion after

3 h of TOS. It was ca. 3-7.5-fold higher compared to extrudates with the uniformly distributed Ru in the entire shaped body (**E-B**, **E-C**, **E-D**). Although the major isomer obtained in citral transformations over extrudates was menthol as in the citronellal case,[1] the stereoselectivity of menthol isomers was significantly different (Figure 11, Table S4). In the citronellal case, the stereoselectivity was the same for all extrudates (70%:20:1%:9% of ME:NME:IME:NIME),[1] while in the citral case, a similar result (ca. 66%:20:0%:14% of ME:NME:IME:NIME) was obtained only over extrudates **E-A**, **E-B** with a random Ru deposition. In the case of **E-C**, **E-D** extrudates with selective Ru deposition, some amounts of isomenthol (Y_{IME} = 0.5%) were also observed with stereoselectivity 38% and 22% for extrudates with Ru deposited exclusively on the Bindzil binder and on H-MCM-41, respectively (Table S4). This is different from a batch experiment over a powder catalyst in citral transformations where isomenthol was observed as the major isomer with stereoselectivity 44-100% (Figure 7, Table S4).

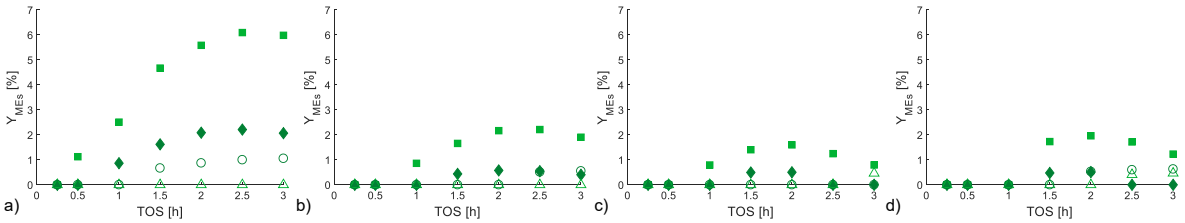

*Figure 11. Menthol isomers as a function of time-on-stream in citral transformations over Ru/(H-MCM-41+Bindzil-50/80) extrudates in the trickle-bed reactor: a) Ru/(H-MCM-41+Bindzil), post synthesis (**E-A**), b) Ru/(H-MCM-41+Bindzil), in-situ synthesis (**E-B**), c) Ru/(Bindzil)+H-MCM-41 (**E-C**), d) Ru/(H-MCM-41)+Bindzil (**E-D**). Conditions: 70 °C, 10 bar of H_2, 0.086 M initial concentration of citral in cyclohexane, 1 g of catalyst, 12.5 min of residence time. Legend: menthol (light green, filled square), neomenthol (dark green, filled diamond), isomenthol (light green, empty triangle), neoisomenthol (dark green, empty circle).*

Furthermore, in line with the literature,[2] Z-citral (neral) was transformed always faster than E-citral (geranial) over all catalysts but with a different rate depending on the catalyst type (Table S5, Figure S8). The initial Z-/E-citral ratio decreased from 1 to 0.22-0.60 and to 0.28-0.64 for powder catalysts and extrudates, respectively (Table S5).

Figures S8a,b, related to the powder catalyst, clearly shows that changes in the Z-/E-citral ratio strongly depends on Ru location and that the yield of menthols increased with decreasing Z-/E-citral ratio. The opposite result was obtained for extrudates in the presence of mass transfer limitations (Figure S8c,d), i.e. the yield of menthols decreased with decreasing the Z-/E-citral ratio and changes in Z-/E-citral ratio (Figure S8c) were significantly different for egg-shell extrudates **E-A** compared to other materials with the uniformly distributed Ru in the entire shaped body (**E-B**, **E-C**, **E-D**).

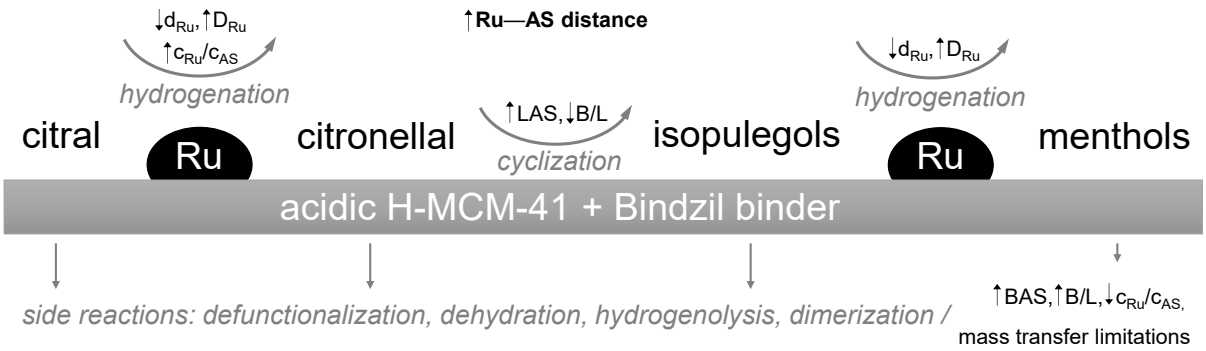

Figure 12. A simplified scheme of menthol synthesis from citral.

The simplified scheme of menthol synthesis from citral (Figure 12) displays rationalization of data obtained in three step transformations of citral over Ru/H-MCM-41 catalyst containing the Bindzil binder. The first step shows that hydrogenation of citral to citronellal requires a small particle size of Ru (d_{Ru}), i.e. a high dispersion (D_{Ru}), and a high ratio of metal-acid sites (c_{Ru}/c_{AS}) (Figure S9). The next step, citronellal cyclization to isopulegols is favored by Lewis acid sites (LAS), i.e. a low ratio of Brønsted to Lewis sites (B/L) (Figures S4, S10), while Brønsted acid sites (BAS), a high B/L, a low c_{Ru}/c_{AS} and the presence of mass transfer limitations are favourable for side reactions (Figure S10). Preferential citronellal cyclization to isopulegols over Lewis acid sites is in line with the studies available in the literature [10,39] when

utilization of non-supported Lewis acids such as $ZnBr_2$ and $ZnCl_2$ afforded > 95% selectivity to isopulegols with stereoselectivity to the desired (±)-isopulegol exceeding 90%. The mechanism proposed for cyclization of citronellal over $ZnCl_2$, a Lewis acid,[40,41] includes coordination of citronellal through oxygen in the carbonyl group and the electron-rich double bond onto the Zr ion bringing citronellal into an orientation favourable for the ring closure. Undesired side-products can be obtained from each step of citral to menthol transformations.[2,4,6,15,22]. In the final step, isopulegols hydrogenation to menthols depends on the particle size of Ru (dispersion) as in the case of the first step. However, the highest yield of menthol over a powder catalyst was obtained over the catalyst with the highest particle size of Ru, but with Ru deposited exclusively on the Bindzil binder, i.e. the longest distance between the active sites of the catalyst (Ru-AS distance) (Figure 5), which turns out to be a key parameter under the kinetic regime. Overall, a relatively low yield of menthol over Ru-catalysts (4.5 – 18.6%) compared to a powder Ni catalysts (54 – 94%)[2-4,6] could be related to the 2.6-fold lower initial hydrogenation rate observed over Ru/H-MCM-41 compared to Ni/H-MCM-41 catalyst in the literature.[2]

4 Conclusions

The Ru-H-MCM-41-Bindzil catalysts with the same composition but different Ru location were prepared in both powder and extrudates form and tested in the one-pot cascade transformations of citral to menthol. For all catalysts, a nominal loading of Ru was 2 wt.% and the weight ratio of H-MCM-41 as a mesoporous acidic material to Bindzil-50/80 as a binder was 70/30. Experiments with the powder catalyst and extrudates were performed with 0.086 M of the initial citral concentration in cyclohexane under 70 °C, 10 bar in the autoclave and the trickle-bed reactor, respectively.

Detailed physico-chemical characterization results confirmed the success of the controlled deposition of Ru giving real Ru loading of 0.9-1.4 wt.% with Ru particle size ranging between 7 and 20 nm. The total acidity of the catalysts was 44-69 μmol/g. After the reaction the surface area and microporosity of catalysts decreased by ca. 23% and 30%, respectively, which can be attributed to coke formation.

In the kinetic regime, Ru location in the powder catalyst affected both activity and selectivity. The best result in terms of citral conversion (58%) and the menthols yield (2.8%) was achieved over the catalyst where Ru was deposited on the Bindzil binder, i.e. with the largest distance between the metal and acid sites, and at the same time with the highest total acidity.

On the contrary, data in the trickle-bed reactor over extrudates showed that location of Ru is minor importance compared to the effect of mass transfer. The best result in terms of citral conversion (70%) and menthols yield (9.1%) was achieved over egg-shell extrudates with Ru distribution at the outermost layer of extrudates, random Ru deposition on both H-MCM-41 and the Bindzil binder, exhibiting the highest Ru dispersion among the studied extrudates. The same catalyst displayed the absolutely highest yield of the desired menthol of 6% with stereoselectivity of 66% at 12.5 min residence time after 3 h of time-on-stream.

Comparison between batch and continuous experiments confirmed the presence of mass transfer limitations in the case of over extrudates. The effectiveness factor for extrudates was calculated to be 0.18 – 0.29. Moreover, significantly differences in the product distribution were observed. For the powder catalysts the presence of citronellal and isomenthol isomer was characteristic, while for extrudates 3,7-dimethyloctan-1-ol, p-menthane and menthol isomer were formed in significant amounts.

5 Supporting Information

Definitions, catalyst characterization data and catalytic testing data.

6 Acknowledgments

The authors are grateful to Academy of Finland for funding through the project: Synthesis of spatially controlled catalysts with superior performance.

7 References

1. Z. Vajglová, N. Kumar, M. Peurla, K. Eränen, P. Mäki-Arvela and D. Y. Murzin, *Catal. Sci. Technol.*, 2020, **10**, 8108-8119.
2. P. Mäki-Arvela, N. Kumar, D. Kubička, A. Nasir, T. Heikkilä, V. P. Lehto, R. Sjöholm, T. Salmi and D. Y. Murzin, *J. Mol. Catal. A-Chem.*, 2005, **240**, 72-81.
3. A. F. Trasarti, A. J. Marchi and C. R. Apesteguia, *J. Catal.*, 2004, **224**, 484-488.
4. A. F. Trasarti, A. J. Marchi and C. R. Apesteguia, *J. Catal.*, 2007, **247**, 155-165.
5. P. Mertens, F. Verpoort, A. N. Parvulescu and D. De Vos, *J. Catal.*, 2006, **243**, 7-13.
6. A. F. Trasarti, A. J. Marchi and C. R. Apesteguia, *Catal. Commun.*, 2013, **32**, 62-66.
7. A. K. Shah, G. Maitlo, A. A. Shah, I. A. Channa, G. A. Kandhro, H. A. Maitlo, U. H. Bhatti, A. Shah, A. Q. Memon, A. S. Jatoi and Y. H. Park, *React. Kinet. Mech. Catal.*, 2019, 1-18.
8. A. Negoi, K. Teinz, E. Kemnitz, S. Wuttke, V. I. Parvulescu and S. M. Coman, *Top. Catal.*, 2012, **55**, 680-687.
9. A. Zuliani, C. M. Cova, R. Manno, V. Sebastian, A. A. Romero and R. Luque, *Green Chem.*, 2020, **22**, 379-387.
10. J. Plösser, M. Lucas and P. Claus, *J. Catal.*, 2014, **320**, 189-197.
11. J. Plösser, M. Lucas, J. Wärnå, T. Salmi, D. Y. Murzin and P. Claus, *Org. Process. Res. Dev.*, 2016, **20**, 1647-1653.
12. P. Mäki-Arvela, N. Kumar, V. Nieminen, R. Sjöholm, T. Salmi and D. Y. Murzin, *J. Catal.*, 2004, **225**, 155-169.
13. U. K. Singh and M. A. Vannice, *J. Catal.*, 2001, **199**, 73-84.
14. P. Mäki-Arvela, L. P. Tiainen, A. K. Neyestanaki, R. Sjöholm, T. K. Rantakyla, E. Laine, T. Salmi and D. Y. Murzin, *Appl. Catal. A-Gen.*, 2002, **237**, 181-200.
15. N. M. Bertero, A. F. Trasarti, B. Moraweck, A. Borgna and A. J. Marchi, *Appl. Catal. A-Gen.*, 2009, **358**, 32-41.
16. A. K. Shah, Y. H. Park, S. Athar, A. Qayoom and M. Choi, *IJCEE*, 2015, **6**.
17. Y. T. Nie, S. Jaenicke and G. K. Chuah, *Chem. Eur. J.*, 2009, **15**, 1991-1999.

18.J. Aumo, S. Oksanen, J. P. Mikkola, T. Salmi and D. Y. Murzin, *Ind. Eng. Chem. Res.*, 2005, **44**, 5285-5290.

19. I. Fatimah, D. Rubiyanto, N. I. Prakoso, A. Yahya, Y-L. Sim, *Sustain. Chem. Pharm.*, 2019, **11**, 61-70.

20.P. Virtanen, H. Karhu, G. Toth, K. Kordas and J. P. Mikkola, *J. Catal.*, 2009, **263**, 209-219.

21.P. Mäki-Arvela, L. P. Tiainen, M. Lindblad, K. Demirkan, N. Kumar, R. Sjöholm, T. Ollonqvist, J. Vayrynen, T. Salmi and D. Y. Murzin, *Appl. Catal. A-Gen.*, 2003, **241**, 271-288.

22.M. Azkaar, P. Mäki-Arvela, Z. Vajglová, V. Fedorov, N. Kumar, L. Hupa, J. Hemming, M. Peurla, A. Aho and D. Y. Murzin, *React. Chem. Eng.*, 2019, **4**, 2156-2169.

23.Z. Vajglová, N. Kumar, P. Mäki-Arvela, K. Eranen, M. Peurla, L. Hupa and D. Y. Murzin, *Org. Process. Res. Dev.*, 2019, **23**, 2456-2463.

24.Z. Vajglová, N. Kumar, M. Peurla, L. Hupa, K. Semikin, D. A. Sladkoyskiy and D. Y. Murzin, *Ind. Eng. Chem. Res.*, 2019, **58**, 10875-10885.

25.Z. Vajglová, N. Kumar, P. Mäki-Arvela, K. Eränen, M. Peurla, L. Hupa, M. Nurmi, M. Toivakka and D. Y. Murzin, *Ind. Eng. Chem. Res.*, 2019, **58**, 18084-18096.

26.Z. Vajglová, N. Kumar, M. Peurla, J. Peltonen, I. Heinmaa and D. Y. Murzin, *Catal. Sci. Technol.*, 2018, **8**, 6150-6162.

27.P. S. F. Mendes, J. M. Silva, M. F. Ribeiro, A. Daudin and C. Bouchy, *J. Ind. Eng. Chem.*, 2018, **62**, 72-83.

28.G. T. Whiting, F. Meirer, M. M. Mertens, A. J. Bons, B. M. Weiss, P. A. Stevens, E. de Smit and B. M. Weckhuysen, *ChemCatChem*, 2015, **7**, 1312-1321.

29.R. V. Jasra, B. Tyagi, Y. M. Badheka, V. N. Choudary and T. S. G. Bhat, *Ind. Eng. Chem. Res.*, 2003, **42**, 3263-3272.

30.F. Dorado, R. Romero and P. Canizares, *Ind. Eng. Chem. Res.*, 2001, **40**, 3428-3434.

31.H. Liu, Y. M. Zhou, Y. W. Zhang, L. Y. Bai and M. H. Tang, *Ind. Eng. Chem. Res.*, 2008, **47**, 8142-8147.

32.M. B. Yue, N. Yang and Y. M. Wang, *ACTA Phys.-Chim. Sin.*, 2012, **28**, 2115-2121.

33.Y. Song, L. L. Zhang, G. D. Li, Y. S. Shang, X. M. Zhao, T. Ma, L. M. Zhang, Y. L. Zhai, Y. J. Gong, J. Xu and F. Deng, *Fuel Process. Technol.*, 2017, **168**, 105-115.

34.X. Wu, A. Alkhawaldeh and R. G. Anthony, in *Studies in Surface Science and Catalysis*, Elsevier Science, 2002, pp. 217-225.

35.P. G. J. Koopman, A. P. G. Kieboom and H. Vanbekkum, *J. Catal.*, 1981, **69**, 172-179.

36.D. Kubička, N. Kumar, T. Venalainen, H. Karhu, I. Kubickova, H. Osterholm and D. Y. Murzin, *J. Phys. Chem. B*, 2006, **110**, 4937-4946.

37.F. Neatu, S. Coman, V. I. Parvulescu, G. Poncelet, D. De Vos and P. Jacobs, *Top. Catal.*, 2009, **52**, 1292-1300.

38.Y. Z. Zhu, Y. T. Nie, S. Jaenicke and G. K. Chuah, *J. Catal.*, 2005, **229**, 404-413.

39. J. T. Williams, P. S. Bahia, B. M. Kariuki, N. Spencer, D. Philip and J. S. Snaith, *J. Org. Chem.*, **2006**, 71, 2460-2471.

40. G. K. Chuah, S. H. Liu, S. Jaenicke and L. J. Harrison, *J. Catal.*, 2001, **200**, 352-359.

41. Y. Nakatani, K. Kawashima, *Synthesis*, 1978, **2**, 147-148.